# Solenoids and Plectonemes in Stretched and Twisted Elastomeric Filaments

A. Ghatak* and L. Mahadevan†

*Division of Engineering and Applied Sciences, Harvard University, Cambridge, 02138 Massachusetts, USA*

(Received 1 April 2005; published 25 July 2005)

We study the behavior of a naturally straight highly extensible elastic filament subjected to large extensional and twisting strains. We find that two different phases can coexist for a range of parameter values: the plectoneme and the solenoid. A simple theory based on a neo-Hookean model for the material of the filament and accounting for the slender geometry suffices to explain these observations, and leads to a phase diagram that is consistent with observations. Extension and relaxation experiments on these phases show the presence of large hysteresis loops and sawtoothlike force-displacement curves which are different for the plectoneme and the solenoid.

DOI: 10.1103/PhysRevLett.95.057801 PACS numbers: 61.41.+e, 46.32.+x, 81.05.Lg

Filamentous structures arise naturally in molecular and cellular biology, polymer physics, ropes, braids, textiles, etc. Long wavelength models for the deformations of these continua take a deceptively simple form wherein filaments are assumed to bend and twist but not stretch or shear transversely. While the assumption of inextensibility and transverse unshearability is certainly a good one in many situations, there is a large class of naturally occurring filaments that are highly extensible: on the molecular scale in multidomain proteins [1], on the mesoscopic scale in fibers [2], and on the macroscale in the context of rubber and gel filaments that deform primarily via shear. Here we consider the mechanics of a naturally straight, highly extensible, elastic rod subjected to extensional and torsional loads, and show that their behavior can be qualitatively different from that of the extensively studied case of inextensible filaments, due to the presence of a new highly packed conformation, the solenoidal phase.

Figure 1(a) depicts the schematic of our experiment in which a soft cylindrical rubber filament of diameter $2a$ and length $L_0$ is stretched vertically by clamping one end to a rigid support and hanging a weight $W$ at the other end. A horizontal bar attached to the weighted end is used to twist the rod about its axis by an angle $\psi L$, $L$ being the deformed length. We find that the filament remains straight [Fig. 1(b)] as long as the twist density $\psi$ is less than a critical value. However, even when the filament is straight, we notice a marked increase in the length as the twist density increases. This coupling between the shear deformations and the normal extension is the result of large strain in highly extensible materials, and is known as the Poynting effect [3]. When $\psi > \psi_c$, the rod buckles into a helical form shown in Fig. 1(b) by switching into one of two compact, packed structures depending on the nominal stretch $\lambda_0 = L/L_0$. When $\lambda_0 \sim O(1)$ we see the plectonemic structure [4] shown in Fig. 1(d) while the preferred state for large $\lambda_0$ is a tightly packed helix or solenoidal form. When the initial stretch is large, a further increase in the twist causes the solenoidal phase to invade the entire filament [Fig. 1(e)] typically nucleating at a boundary leading to a secondary structure that is itself filamentlike, albeit with very different mechanical and geometrical properties. On twisting still further, tertiary solenoidal and plectonemic structures begin to appear as shown in Fig. 1(g). These knurled structures are the basis for the

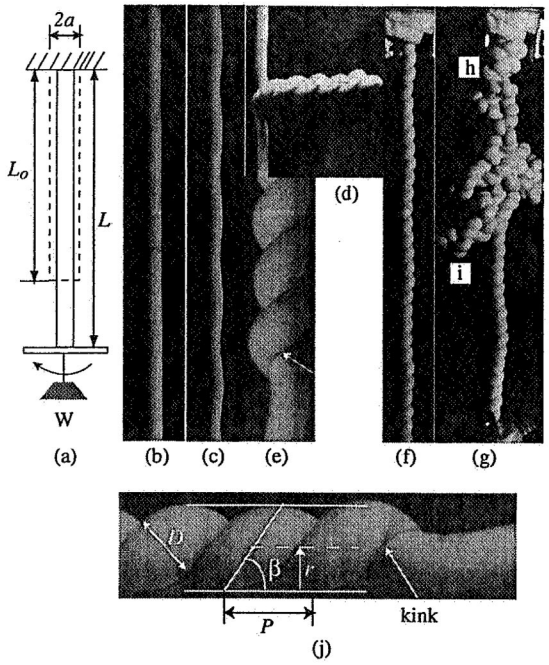


FIG. 1. (a) The experiment consists of clamping a rubber rod to a rigid support, which is then stretched by hanging a weight $W$ and is twisted about its axis by rotating a bar attached to the weight. (b) For small to intermediate values of the twist, the rod remains straight while its length increases. (c) Beyond a threshold in the twisting strain, the straight configuration loses stability to a helical form. Depending on the initial extension, we see (d) the plectonemic phase or (e) the solenoidal phase. For the solenoidal phase, as the twist is increased still further, the whole rod is converted to (f) a solenoidal structure, which is then transformed into (g) tertiary structures that are constituted of both (h) higher-order solenoidal and (i) plectonemic structures. In (j) we show our notation and point out the appearance of kinks at the junction between the straight and solenoidal parts of the filament.

 

typical appearance of wools and certain textiles [5]. Although related observations have been made earlier [4,6–8], the experimental and theoretical analysis of the solenoidal structures and their coexistence with plectonemes is new.

The configuration of the filament is determined by minimizing the free energy of the system which is the sum of the stretching ($\Pi_S$), twisting ($\Pi_T$), and the bending energy ($\Pi_B$) of the rod and the potential energy ($\Pi_W$ and $\Pi_M$) of the external load. We note that for the straight part of the filament, the controlling parameters are the extensional load $W$ and the twist density $\psi$. However, for the solenoid the controlling parameters are the end load $W$ and torque $M$, owing to the softness of the intervening twisted filament which effectively transmits loads (extensional and torsional) rather than displacements. If the subscript $s$ characterizes the part of the rod that is transformed into a solenoid so that $L_s$ is the length of the solenoidal phase in the undeformed (reference) configuration, we may write

$$\Pi_S = (C/a^2)[L_s J_s + (L_0 - L_s)J], \tag{1}$$

$$\Pi_T = (C/2a^2)[L_s\lambda_s(\bar{\psi}_s a)^2 + (L_0 - L_s)\lambda(\psi a)^2], \tag{2}$$

$$\Pi_B = (BL_s/2\lambda_s)(\sin^4\beta/r^2), \tag{3}$$

where $B = \pi a^4 E/4$ is the bending rigidity of the rod, and $C = 2B/3$ is the twisting rigidity of the rod (assumed to be incompressible). Equation (1) follows from the mechanical energy density for an incompressible neo-Hoookean material in pure extension [9], with $J = (\lambda^2 + 2/\lambda - 3)$. Here $\lambda$ is the true stretch which is coupled to the shear due to twist [3]. In a force controlled experiment as here, the true stress in the absence of any twist $(E/3)$ $(\lambda - 1/\lambda_0{}^2)$ is the same as the stress in the presence of twist [9] $(E/3)$ $(\lambda_0 - 1/\lambda^2 - (\psi a)^2/4)$. In terms of the function $f(\lambda) = \partial J/\partial\lambda = \lambda - 1/\lambda^2$ we may thus write the true stretch in terms of the nominal stretch $\lambda_0$, and the twist strain $\psi$ as:

$$f(\lambda) = f(\lambda_0) + (\psi a)^2/4. \tag{4}$$

Equation (2) follows from the twist energy for a helical filament with helix angle $\beta$, radius $r$ [Fig. 1(e)], and total twist density [10] $\bar{\psi}_s = \psi_s + \sin\beta\cos\beta/r$, while Eq. (3) is the bending energy of the solenoidal helix with curvature $\sin^2\beta/r$. The potential energy of the dead load $W$ and the torque $M = C\psi$ are

$$\Pi_W = W[L_s(1 - \lambda_s\cos\beta) + (L_0 - L_s)(1 - \lambda)] \tag{5}$$

$$\Pi_M = -M[L_s\lambda_s(\psi_s + \sin\beta/r) + (L_0 - L_s)\lambda\psi]. \tag{6}$$

The expressions for the energy written above are similar to those for helical springs [4,10] with the important qualitative difference associated with the finite extensibility of the rod, an effect at the root of all the new phenomena described here. In deriving the above expressions, we have used a characterization of the solenoid as a perfect helix of circular cross section, thus neglecting the effects of self-contact, and have also neglected the effects of the kinks at the junction between the solenoidal and the straight part of the filament where the twist density and the rod diameter change discontinuously.

Extremizing the total energy $\Pi(\psi, \psi_s, \beta, r) = \Pi_W + \Pi_M + \Pi_S + \Pi_T + \Pi_B$ with respect to $\psi_s$ yields

$$M = C\psi = C\bar{\psi}_s, \tag{7}$$

which implies that the twist density is conserved in the straight and the helical part of the rod. Similarly, extremizing $\Pi$ with respect to $\beta$ and $r$ yields

$$\begin{aligned} M &= C\cos\beta\bar{\psi}_s + \frac{B\sin^3\beta}{r\lambda_s^2} \\ W &= \frac{C\bar{\psi}_s\sin\beta}{r} - \frac{B\sin^2\beta\cos\beta}{(r\lambda_s)^2}. \end{aligned} \tag{8}$$

Finally, substituting (7) in (8) yields expressions for the radius of the helix $r$ and the twist density of the helical solenoid $\psi_s$ in terms of the load $W$ and the helix angle $\beta$:

$$r = \sqrt{\frac{B}{W}}\frac{\sin\beta}{\lambda_s}, \qquad \psi_s = \sqrt{\frac{W}{B}}\left(\frac{3(1 + \cos\beta)}{2\lambda_s} - \lambda_s\cos\beta\right). \tag{9}$$

We thus have six equations (7)–(9) for eight unknowns: $W$, $M$, $\beta$, $r$, $\psi$, $\psi_s$, $\lambda$, and $\lambda_s$. We solve these equations by assuming a value for the dead load $W$ and the helix angle $\beta$ and determine $r$, $\psi_s$, and $\lambda_s$. For each $W$, the range of allowable $\beta$ is limited to $(0, \beta_m)$, with the latter limit corresponding to the case when there is self-contact, which occurs when the helix pitch $P = 2\pi r/\tan\beta_m$ is equal to the diameter of the stretched rod $D = 2a/\sqrt{\lambda_s}$. In Fig. 2 we plot $\beta$ with respect to $\lambda$ thus calculated for a range of extensional loads $W = 0.6$–$6.5$ N. Since the filament twist must be in the same direction for both the straight and the solenoidal parts of the filament, it follows from Eq. (9) that $3(1 + \cos\beta)/2\lambda_s \geq \lambda_s\cos\beta$. Therefore, we must exclude the set of values of $\beta$ for which $\psi_s < 0$ [11]. In Fig. 2, $\beta \in [0, \beta_m]$ for curves 1–4, while for curve 5 $\beta \in [14°, \beta_m]$, in accordance with this constraint.

The solutions depicted in Fig. 2 are stable if all the eigenvalues of the Hessian matrix $\frac{\partial^2\Pi}{\partial a_i\partial a_j}|_{a_k, k\neq i,j}$ with $a_i = \beta$, $\psi_s$, and $r$ remain positive. For all $W$, when $\beta < \epsilon \approx 3°$ the Hessian matrix is positive definite, signifying that the straight rod remains straight for small perturbations. However, for all sets of solutions with $\beta > \epsilon$, one of the three eigenvalues is negative, implying that these solutions are unstable. The dashed lines 1–5 signify that these solutions are saddle points so that a straight filament with $\beta = 0$ becomes unstable for perturbations that are large enough and transitions suddenly to a solenoidal shape with $\beta = \beta_m$. Experimentally we typically see the appearance

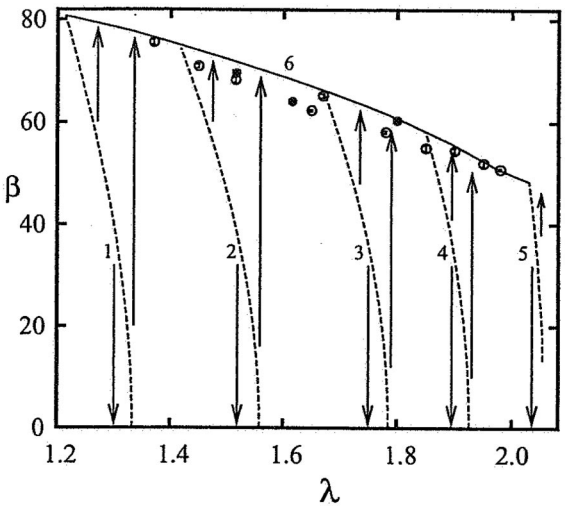


FIG. 2. Equilibrium values of the solenoid angle $\beta$ [obtained from (8)] vs the stretch $\lambda$ for different extensional loads $W$. The curves 1 to 5 correspond to rubber rod with $2a = 3.75$ mm subjected to $W = 0.6$, 1.5, 3.0, 4.4, and 6.4 N, respectively. Curve 6 represents the upper limit of the solenoid angle $\beta_m$ when the helix pitch $P = D$ the diameter of the stretched filament. The $\beta_m$ data from experiments are also plotted with respect to $\lambda$. Symbols ○ and ● represent rubber rods of elastic modulus $E = 1.3$ MPa and diameter $2a = 3.175$ and 6.35 mm, respectively.

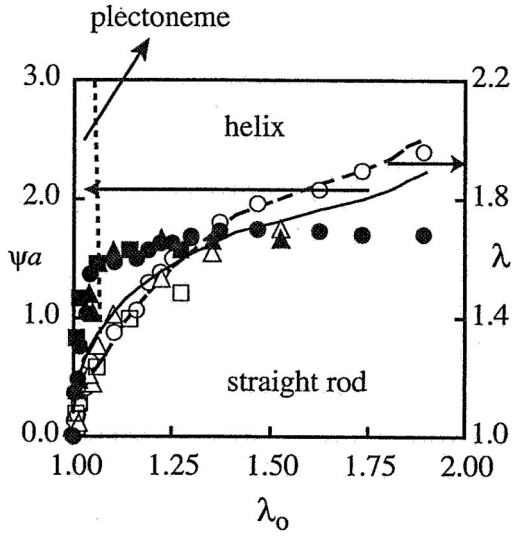


FIG. 3. Phase diagram. The dimensionless twist density $\psi a$ (filled symbols) at which the plectoneme/solenoidal phase arises are plotted with respect to the initial extension ratio $\lambda_0$ of the rod. The solid line represents the theoretical transition curves for $\psi a$ while the dashed line represents the transition curve for $\lambda$ as a function of $\lambda_0$ calculated using (4)–(9). The "circles" correspond to filaments of modulus $E = 1.3$ MPa and diameter $2a = 3.175$ mm, the "triangles" correspond to $2a = 6.35$ mm, and the squares correspond to $E = 2.6$ MPa and $2a = 6.35$ mm. The vertical dashed line separates the plectoneme and the straight phase, while the solid line separates the straight phase from the solenoidal phase.

of a number of coils simultaneously due to the strongly subcritical nature of the transition.

In Fig. 3 we plot the critical twist density (filled symbols) at which a straight filament subjected to the initial extension ratio $\lambda_0$ transforms either to a plectoneme or to a helix. When the initial extension is small, $\lambda_0 < 1.1$, corresponding approximately to the case of an inextensible filament, twisting the straight rod sufficiently results in the plectonemic phase. However, the solenoidal tightly coiled helix nucleates when $\lambda_0 > 1.1$. The open symbols in this figure represent the corresponding experimentally obtained stretch $\lambda$ of the filament at which this phase transition occurs. We also plot the theoretical curves of the critical twist density and the extension ratios as obtained by solving Eqs. (4)–(9) along with the constraint that the solenoid angle $\beta_m$ is achieved with the helix pitch $P = D$. Although $P$ remains slightly larger than $D$ with $P/D = 1.1 \pm 0.1$ for the whole range of $W$, the experiments agree with the simple theory over a range of $\lambda$.

A consequence of the subcritical transition to the packed solenoidal structures is that they unwind at a load higher than that when formed. Indeed we observe this hysteresis if we first nucleate the solenoidal phase and then stretch the rod in a displacement-controlled experiment to unwind them while keeping the total number of turns constant. In a cyclic experiment, the results of which are shown in Fig. 4 (curve 2), the solenoidal helices unwind progressively with an increase in extension but they reappear at a different value of the extension during relaxation. The size of the hysteresis loop increases with the initial load $W_0$. Figure 4 depicts the load-displacement history for different initial loads, $W_0 = 0.1$–1.0 N. As the displacement $\Delta$ is increased, curve 2 shows how the tightly packed helical coils straighten out one by one with the solenoid angle $\beta$ jumping from $\beta_m$ to zero with a concomitant sharp drop in the load. Similarly, when the extension is relaxed, helices start to appear one by one with sharp increases in the load associated with the formation of individual coils. The resulting sawtooth pattern for the $W - \Delta$ curve persists even after repeated extension-relaxation cycles. An approximate estimate of the spacing between the peaks can be deduced from the axial increase in length due to the unwinding of a single helical pitch $\Delta d = (1 - \cos\beta)\Delta L$ where $\Delta L = 2\pi r/\sin\beta = 2\pi/\lambda_s\sqrt{B/W}$ is the contour length of a pitch. For curve 2, using $2a = 3.75$ mm, $E = 1.3$ MPa, $W_0 = 2.0$ N, and $\beta = 70°$, $\lambda_s = 1.3$ we find that $\Delta d = 9.25$ mm, consistent with the experimentally obtained mean value of $10.5 \mp 1$ mm. The drop in load during the extension or relaxation of a helical pitch also depends upon the load $W$; small $W$ result in a large $\Delta d$ and thus a more pronounced sawtooth. For comparison, we also show the graph for a straight untwisted filament (curve 1) which follows the qualitatively different hysteretic behav-

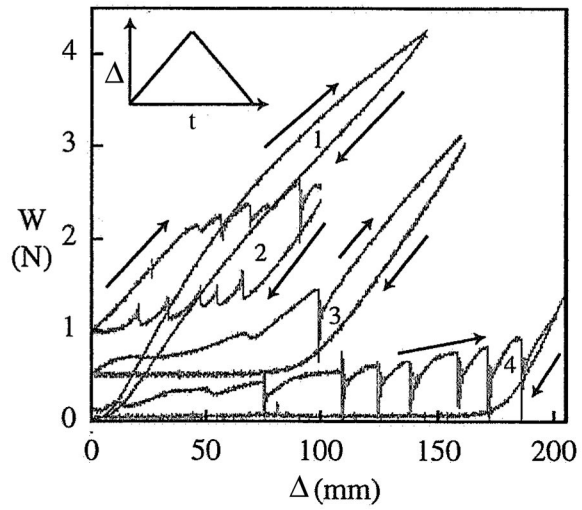


FIG. 4. The force-extension response of a rubber filament during a cycle or loading and unloading displacements (see triangular ramp). Curve 1 depicts the response of a straight filament which is simply stretched. Curve 2 represents that for a filament with a series of solenoids (initial load $W_0 = 1.0$); as the load increases, the solenoids unwind leading to sawtoothlike response. Curves 3 represent the response of a single plectoneme (initial load $W_0 = 0.5$) while curve 4 ($W_0 = 0.1$ N) represents the response of a multiple-plectoneme filament; here the sawtoothlike structure corresponds to the unwinding of the loop at the end of the plectoneme that is similar to a solenoidal structure when stretched. Observe the marked difference between the unloading curves for the solenoidal filament (2) and the plectoneme (3) and (4); the latter are smooth while the former show a sawtoothlike response. All the experiments were carried out keeping the total twist constant, and with filaments of diameter $2a = 3.75$ mm and modulus $E = 1.3$ MPa.

ior characteristic of elastomeric materials, in contrast with the hysteresis induced by the complex geometry of the helix/solenoidal phases that yields curve 2.

The response of a single plectonemic structure is presented in curve 3 of Fig. 4. We see that the individual helices of the plectoneme unwind continuously until the very last one when a sharp drop in the force is observed. While the continuous change in load corresponds to supercritical growth of the plectoneme, the last drop in the load arises because the loop at the end of a plectoneme is similar to a solenoidal coil. During relaxation the plectoneme does not reappear leading to a single solenoidal coil; this is consistent with the subcritical nature of plectoneme formation in extensible filaments in a load controlled situation like here. Finally, if multiple plectonemes are artificially introduced while twisting the straight rod, the force-displacement curve is smooth initially until the last part of each plectoneme, a solenoidlike structure—this leads to the sawtooth pattern seen in curve 4, but during relaxation there are no jumps, as expected. Thus we see that the extension-relaxation cycles of the plectoneme and solenoidal structures result in distinctly different load-displacement diagrams and could be used as a signature of the secondary and tertiary structure of twisted filaments; i.e., they are essentially dictated by geometrical structures rather than material properties.

The jagged load-displacement curves in Fig. 4 are reminiscent of similar patterns observed in stretching experiments on single molecules and on natural fibers. However, there is a qualitative difference between our macroscopic experiments and those on the molecular scale—while for proteins the sawtoothlike response corresponds to unfolding of individual domains held together by short range forces, in the macroscopic experiment, the response happens due to unwinding of plectonemic or helical coils formed under extensional and torsional end loads, and is thus due more to geometry. This hysteretic behavior forms the basis for the extensibility of matted and knotted wool and other fibrous materials, a subject worthy of further study.

We acknowledge the support of the Office of Naval Research through the Young Investigator Program and the Schlumberger Chair Fund at Cambridge University (L. M.) where this work was begun.

*Email: aghatak@iitk.ac.in
†Email: lm@deas.harvard.edu

[1] M. Rief *et al.*, Science **276**, 1109 (1997).
[2] N. Becker *et al.*, Nat. Mater. **2**, 278 (2003).
[3] J. H. Poynting, Proc. R. Soc. London **82**, 546 (1909).
[4] J. M. T. Thompson and A. R. Champneys, Proc. R. Soc. A **452**, 117 (1996).
[5] J. W. S. Hearle, P. Grossberg, and S. Backer, *Structural Mechanics of Fibers, Yarns and Fabrics* (Wiley, New York, 1969).
[6] A. A. Travers and J. M. T. Thompson, Phil. Trans. R. Soc. A **362**, 1265 (2004).
[7] A. N. Gent and K.-C. Hua, Int. J. Non-Linear Mech. **39**, 483 (2004).
[8] S. Przybyl and P. Pierański, Eur. Phys. J. E **4**, 445 (2001).
[9] R. S. Rivlin, Phil. Trans. R. Soc. A **240**, 509 (1948).
[10] A. E. H. Love, *A Treatise on the Mathematical Theory of Elasticity* (Dover, New York, 1926), pp. 414–415.
[11] For an inextensible rod ($\lambda_s = 1$), for which $\psi_s = \sqrt{W/B}(1 + \cos\beta)/2$ remains positive for all values of $\beta$.